

Exosome mimetics derived from bone marrow mesenchymal stem cells deliver doxorubicin to osteosarcoma *in vitro* and *in vivo*

Jinkui Wang^{a,b,c,d,e,f,t}, Mujie Li^{a,b,c,d,e,f,t}, Liming Jin^{a,b,c,d,e,f}, Peng Guo^g, Zhaoxia Zhang^{a,b,c,d,e,f}, Chenghao Zhanghuang^{a,b,c,d,e,f}, Xiaojun Tan^{a,b,c,d,e,f}, Tao Mi^{a,b,c,d,e,f}, Jiayan Liu^{a,b,c,d,e,f}, Xin Wu^{a,b,c,d,e,f}, Guanghui Wei^{a,b,c,d,e,f} and Dawei He^{a,b,c,d,e,f}

^aDepartment of Urology, Children's Hospital of Chongqing Medical University, Chongqing, P.R. China; ^bChongqing Key Laboratory of Children Urogenital Development and Tissue Engineering, Children's Hospital of Chongqing Medical University, Chongqing, P.R. China; ^cChongqing Key Laboratory of Pediatrics, Children's Hospital of Chongqing Medical University, Chongqing, P.R. China; ^dMinistry of Education Key Laboratory of Child Development and Disorders, Children's Hospital of Chongqing Medical University, Chongqing, P.R. China; ^eNational Clinical Research Center for Child Health and Disorders, Children's Hospital of Chongqing Medical University, Chongqing, P.R. China; ^fChina International Science and Technology Cooperation Base of Child development and Critical Disorders, Children's Hospital of Chongqing Medical University, Chongqing, P.R. China; ^gInstitute of Basic Medicine and Cancer (IBMC), Chinese Academy of Sciences, Hangzhou, Zhejiang, China

ABSTRACT

Osteosarcoma is a bone tumor with a high incidence in children and adolescents. Chemotherapy for osteosarcoma is limited, and effective targeted drugs are urgently needed to treat osteosarcoma. Exosomes as a natural nano drug delivery platform have been widely studied and proven to have good drug delivery performance. However, the low production of exosomes hinders its development as a carrier. Exosome mimetics (EMs) as an alternative product of exosomes solve the problem of low production of exosomes and maintain the good performance of exosomes as carriers. In this study, bone marrow mesenchymal stem cells (BMSCs) were sequentially extruded to generate EMs to encapsulate doxorubicin (EM-Dox) to treat osteosarcoma. The results showed that we successfully prepared EMs of BMSC, and EM-Dox was prepared using an active-loading approach. Our engineered EM-Dox demonstrated significantly more potent tumor inhibition activity and fewer side effects than free doxorubicin. This novel biological nanomedicine system provides a promising opportunity to develop novel precision medicine for osteosarcoma.

ARTICLE HISTORY

Received 9 September 2022
Revised 18 October 2022
Accepted 25 October 2022

KEYWORDS



Bone marrow mesenchymal stem cells; exosome mimetics; doxorubicin; osteosarcoma; drug delivery

1. Introduction

Osteosarcoma is the most common malignant tumor originating from bone tissue (Zhang et al., 2021), more frequently occurring in children and adolescents. To date, surgical resection in combination with neoadjuvant chemotherapy is the standard-of-care treatment for osteosarcoma. Unfortunately, the 5-year survival rate of patients with osteosarcoma was only 60%–70% (Anninga et al., 2011; Meyers, 2015). Besides, the recurrence rate of patients with osteosarcoma after treatment is still high (Jaffe, 2009; Freyer & Seibel, 2015). One of the reasons is that the chemotherapy drugs currently used for osteosarcoma lack specificity, potency, and have strong off-target side effects. Therefore, there is an urgent and unmet need for developing novel precision medicines with better tumor-killing efficacy and lower side effects to prolong osteosarcoma patients' survival.

Nanosystems have natural advantages as drug delivery systems, such as long circulation time, small size, and tumor aggregation. Li et al. (2020) treated advanced osteosarcoma

with apatinib encapsulated by hydrophobic poly(ester amide) nanoparticles, significantly inhibiting tumor growth with very low side effects. Another study used polymeric nanoparticles to deliver NSC23766 to target the Rac1 pathway to improve prostate cancer treatment (Li et al., 2022). In recent years, exosomes (Exos) have become a promising way to deliver chemotherapy drugs for cancer therapy (Wu et al., 2022). Exos are nanoscale extracellular vesicles secreted by cells and widely present in various cells (Liu, Xia et al., 2021). The primary function of Exos is to maintain the normal metabolism of cells and mediate communications between cells (Song et al., 2021). In addition, Exos involve in many pivotal biological processes and carry out the material exchange between cells by transporting intracellular substances (Li & Wang, 2021). Since Exos are endogenous vesicles with potential natural drug carrier function, they have been intensely investigated as a novel therapeutic modality (van Niel et al., 2018). Because of their low immunogenicity, cyclic stability, inherent targeting and crossing biological barriers, Exos are becoming an effective way to deliver drugs (Alvarez-Erviti

CONTACT Dawei He  hedawei@hospital.cqmu.edu.cn  Department of Urology, Children's Hospital of Chongqing Medical University; 2 ZhongShan Rd, Chongqing 400013, Chongqing, China.

[†]Jinkui Wang and Mujie Li contributed equally to this work and should be considered co-first authors.

© 2022 The Author(s). Published by Informa UK Limited, trading as Taylor & Francis Group.

This is an Open Access article distributed under the terms of the Creative Commons Attribution-NonCommercial License (<http://creativecommons.org/licenses/by-nc/4.0/>), which permits unrestricted non-commercial use, distribution, and reproduction in any medium, provided the original work is properly cited.

et al., 2011; Jiang et al., 2017; Zhu et al., 2019). However, it is still a significant challenge and thorny problem for the current technology to obtain highly purified Exos (Shu et al., 2020). In particular, due to the insufficient number of natural Exos secreted by cells, the large-scale production of Exos is still challenging (Reiner et al., 2017; Colao et al., 2018). In addition, the drug delivery efficiency of Exos as drug carriers is also an unsolved problem (Chen et al., 2021). Therefore, as an alternative to Exos, exosome mimetics (EMs) have higher yields, maintain the same biological functions as Exos, and gradually become a more promising drug delivery nano-platform. In previous studies, cell-derived EMs have been produced by sequential extrusion of cells (Jang et al., 2013; Goh, Zou et al., 2017; Guo et al., 2021). The EMs produced by this method retains the function of Exos to deliver chemotherapeutic drugs with a high yield. However, to date, there is still a lack of studies on EMs as a drug delivery system for osteosarcoma.

EMs as drug delivery carriers have many advantages over existing synthetic systems. First, EMs can naturally target their source sites. We selected EMs of bone marrow mesenchymal stem cells (BMSCs) as drug delivery carriers to target osteosarcoma. Second, the phospholipid bilayers of EMs can fuse with the cell membrane to promote the internalization of encapsulated drugs. Third, the small size of the exosome mimetics promotes its extravasation in tumor blood vessels and diffusion into tumor tissue. Doxorubicin is one of the first-line chemotherapeutic drugs for osteosarcoma. Because of its high toxicity, the clinical application dose of doxorubicin is greatly limited (Gomari et al., 2019). This study aimed to develop EMs derived from BMSCs to deliver doxorubicin for osteosarcoma therapy (Figure 1). We used sequential extrusion to produce EMs and doxorubicin-encapsulating EMs (EM-Dox). Subsequently, we utilized the inherent tumor-homing ability of EMs derived from BMSC to target osteosarcomas; EM-Dox was used to treat osteosarcoma *in situ* xenografts. We hypothesized that the EM-Dox could significantly reduce the side effects of doxorubicin, improve the tumor-homing efficiency, and increase antitumor efficacy.

2. Materials and methods

2.1. Cell culture

Human osteosarcoma cells MG63, and human BMSC lines used in this study were purchased from the Cell Bank of the Chinese Academy of Sciences (Shanghai, China). Human osteosarcoma cells 143B were purchased from China Concord Cell Library (Beijing, China). These cells were cultured in Gibco Dulbecco's Modified Eagle Medium (DMEM) supplemented with 10% fetal bovine serum (FBS), 100 µg/mL streptomycin, and 100 unit/mL penicillin. All cells were cultured in an incubator at 37°C and 5% CO₂. All media and reagents for cell culture were purchased from Gibco (Carlsbad, CA, USA).

2.2. Preparation of Exos, EMs, and EM-Dox

Adherent cells were isolated by scraping, and the collected BMSCs were re-suspended in phosphate-buffered saline (PBS) at a concentration of 5×10^6 cells/mL. The Extruder (Avanti Mini-Extruder) was used for two sequential extrusions through a 10-µm and 5-µm polycarbonate membrane filter (Whatman), as in the previous article (Jang et al., 2013). Then super centrifuged at 100,000g for 70 min and re-suspend in 240 mM ammonium sulfate solution. The monodisperse nanoscale EMs were then prepared using a miniature extruder (Avanti Mini-Extruder) through a 1-µm polycarbonate membrane filter (Whatman). Then slide-A-Lyzer Nutritional Cassette (MWCO 20 kDa) was used overnight at room temperature at 2L PBS (pH7.4) to remove ammonium sulfate outside EMs and form an ammonium sulfate concentration gradient. Then doxorubicin was added to EMs with a concentration of 10^{10} particles/mL at a final concentration of 0.2–1 mg/mL and incubated at room temperature for 6 h to promote the loading of doxorubicin into EMs. The preparation method of ammonium sulfate was described in previous literature (Guo et al., 2021). A doxorubicin-encapsulating EM (EM-Dox) solution was injected into slide-A-Lyzer Nutritional Cassette (MWCO 20kDa) and dialyzed in PBS (pH7.4) overnight at room temperature to remove free doxorubicin. We used the same method to

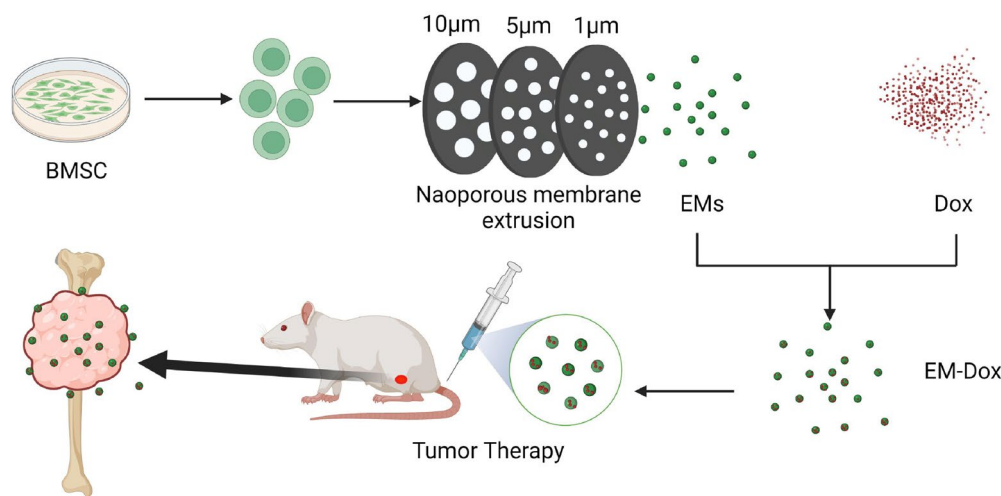


Figure 1. Representative scheme for EM-Dox preparation and treatment of EM-Dox against osteosarcoma of the tibia.

prepare the blank EMs using a miniature extruder (Avanti mini-extruder) through a 10- μ m, 5- μ m, and 1- μ m polycarbonate membrane filter (Whatman) for three sequential extrusions.

At the same time, natural Exos was prepared as control, and Exos of BMSC was separated by supercentrifugation. First, the FBS will be centrifuged at 100,000g for 10 h to deplete Exos in the serum for BMSC cell culture. BMSCs were cultured using DMEM with 10% FBS-depleted Exos for 48 h. Supernatants of cultured cells were collected simultaneously as scraping BMSCs. The collected supernatant was centrifuged to separate Exos. The specific steps are as follows: First, centrifuge the supernatant at 300g for 10 min, 2000g for 20 min, and 10,000g for 30 min, respectively, to remove cells and debris. Then, the supernatant was centrifuged at 100,000g for 70 min to collect the underlying solution and centrifuged again at 100,000g for 70 min. Finally, the separated Exos was re-suspended with a small amount of PBS and placed in a -80°C refrigerator for subsequent research.

2.3. Characterization of Exos, EMs, and EM-Dox

The morphologies of EMs, Exos, and EM-Dox were detected by transmission electron microscopy (TEM). Pierce BCA protein assay determined protein concentrations of EMs, Exos, and EM-Dox. The isolated EMs, Exos, and EM-Dox (4 μ L containing 100 μ g/mL total protein) were adsorbed onto a quantitative foil-hole carbon grid (Spi supplied). The grid was then imaged using a FEITECNAIG2 transmission electron microscope, and images were taken using an AMT2kCCD camera. Particle sizes and concentrations of EMs, Exos, and EM-Dox were analyzed using the ZetaView Nanoparticle tracking analyzer (Particle Metrix, Germany).

2.4. The encapsulation efficiency of doxorubicin

Doxorubicin was quantified using a multi-mode Microplate Reader (Thermo Fisher Technologies, USA), and the excitation and emission wavelengths were 480 nm and 594 nm, respectively (Gomari et al., 2019). Free doxorubicin was used to make a standard curve. The content/concentration of doxorubicin in EM-Dox was calculated according to the curve, and we figured the drug loading rate. We used the following formula to calculate the drug encapsulated effect (EE). $\text{EE} = \text{total doxorubicin loaded in EMs} / \text{total doxorubicin initially added}$.

2.5. The in vitro release of doxorubicin from EMs

EM-Dox (1 mL) was put into slide-A-Lyzer Nutritional cassette (MWCO 20 kDa) and put into PBS (150 mL; pH 7.4 or 5.5), dialyzed at 37°C , and stirred at 100 rpm. The dialysate was absorbed in 0, 3, 6, 9, 12, 24, and 48 h to determine the concentration of doxorubicin release, and we supplemented the same volume of PBS. Doxorubicin quantification, as described earlier, was determined using a multi-mode Microplate Reader.

2.6. Stability of nanosystem

To evaluate the stability of the nanosystem and determine the effect of storage temperature on the size of EM-Dox, EM-Dox was placed at 4°C or room temperature, respectively. Dynamic light scattering (DLS) and zeta potential determinations were performed with a Zetasizer nanoseries instrument (Malvern Nano-Zetasizer). The particle size distribution and zeta potential of EM-Dox under different storage conditions were measured at 1, 2, 3, 5, and 7 days. At the same time, we measured the doxorubicin leakage rate at different storage temperatures. Specifically, we injected 1 mL of EM-Dox into slide-A-Lyzer Nutritional cassette (MWCO 20 kDa) and placed it in PBS (150 mL; pH 7.4). The leakage rate of doxorubicin was determined at room temperature or 4°C . The leakage rate (%) = released doxorubicin content/total doxorubicin content in EM-Dox.

2.7. EMs labeling and uptake studies

Confocal microscopy was used to co-locate EMs, doxorubicin, and cells. The specific methods were as follows: fluorescence dye PKH26 (Sigma-Aldrich, St. Louis, Missouri, USA) was used to label 50 μ L EM-Dox (total protein 20 μ g/mL), mixed EM-Dox with Diluen C, and added to PKH26 for incubation at room temperature for 15 min. We added the same volume medium, and the free dye was removed by supercentrifugation. 143B and MG63 were inoculated in 24-well plates (2×10^4 cells/well), and 25 μ g of labeled EM-Dox was added to each well. After 1, 6, and 9 h, cells were rinsed with PBS, then fixed with 4% paraformaldehyde, and the nuclei were stained by Sigma-Aldrich staining. Results were observed using an inverted fluorescence microscope (Nikon AX, Tokyo, Japan).

2.8. In vitro cytotoxicity assay

The free doxorubicin and EM-Dox cytotoxicity in 143B and MG63 cells was determined using Cell Counting Kit-8 (CCK8). In brief, 143B and MG63 cells were inoculated in a 96-well plate at a density of 2000 cells per well. After cell adherence, we added all cells to a 100 μ L medium, and the drug (free doxorubicin or EM-Dox) was incubated for 24 h. The final concentrations of doxorubicin in the drug were 0, 0.25, 0.5, 1, 2.5, 5, 10, and 15 μ g/mL. Add 10 μ L of CCK8 reagent and incubate at 37°C for 2 h. The absorbance was measured using an ELx800 microplate reader (BioTek, Vermont, USA) at 450 nm. Cells without drugs were used as 100% control, and the CCK8 reagent without cells was blank. We calibrated the spectrophotometer to zero absorbance. All experiments were repeated three times, and the IC₅₀ of free doxorubicin and EM-Dox in osteosarcoma cells was evaluated and compared (Kim et al., 2016).

2.9. In vivo biodistribution experiment

The 5-week-old male BALB/c nude mice were purchased from Huachuang sino Medical Technology Company (Jiangsu, China). The Animal Ethics Committee approved all animal

experiments involved in this study at the children's Hospital Affiliated with Chongqing Medical University. DiR-labeled EMs ($n=3$) or liposomes ($n=3$) (1.5 mg/kg DiR, $\sim 3 \times 10^{10}$ particles/animal, 150 μ L) were intravenously injected into the tail of *in situ* tumor-bearing BALB/c nude mice. The fluorescence in mice was measured by *in vivo* imaging systems (IVIS) Lumina II system (Caliper, Hopkinton, MA, USA) for 6, 24, and 48 h after injection. Then the mice after 48 h were sacrificed, and the fluorescence of the tumor resected in the mice was measured and compared. In addition, the fluorescence intensity of the heart, liver, spleen, lung, and kidney was measured.

2.10. Pharmacokinetic (PK) study

Male Wistar rats (275 \pm 5 g) were purchased from Chongqing Medical University Animal Experiment Center. Five rats received a single intravenous injection of 3 mg/kg of EM-Dox. At 30 min, 1, 2, 4, 8, 24, and 48 h, the plasma was harvested from rats. The blood sample was immediately centrifuged at 3000 rpm/min for 15 min to obtain plasma. Doxorubicin concentration in all plasma was determined by high performance liquid chromatography (HPLC). Pharmacokinetic parameter analysis was done using noncompartmental analysis (WinNolin software version 5.2, Pharsight, Mountain View, CA).

2.11. *In vivo* antitumor activity

The human osteosarcoma cell line (143B, 1×10^6 cells in 100 μ L of PBS) was transplanted into the right hind tibia for *in situ* xenotransplantation. After seven days of tumor cell inoculation, mice were randomly divided into four groups ($n=6$) and treated with EM-Dox (3 mg/kg), free doxorubicin (3 mg/kg), blank EMs (3 mg/kg), and PBS, respectively. Caudal vein injection was administered every three days for four sequential times. Tumor disease was measured every two days during administration using vernier calipers to plot tumor volume–time curves to evaluate *in vivo* antitumor efficacy. The calculation formula of tumor volume (V) is as follows:

$$V = \frac{4\pi}{3} \left(\frac{AP + L}{4} \right)^2$$

AP(apically) is the distance on both sides of the knee cap, and L is the length in front of the tibia where the tumor grows the most (Li et al., 2018). After the fourth treatment, limbs with tumor were collected and weighed. The blood of the mice was collected, and we detected the blood routine, liver function, kidney function, and myocardial enzyme spectrum to observe the organ injury of the mice. Creatine kinase (CK) and lactate dehydrogenase (LDH), urea, Crea, Alanine aminotransferase (ALT), and Aspartate aminotransferase (AST) were measured using assay kits (Rayto, China).

2.12. Statistical analysis

Data were expressed as mean \pm standard deviation (SD) and analyzed by GraphPad Prism 8 (GraphPad Software).

Differences between groups were compared using the Student T test. One-way ANOVA was used for statistical comparison among different groups. p values less than .05 were considered a significant difference between groups.

3. Results

3.1. Preparation and characterization of EMs and EM-Dox

We prepared EMs by sequential extrusion of BMSCs according to an established method (Jang et al., 2013). The EMs were characterized by TEM, demonstrating a spherical lipid bilayer vesicle appearance of 30–200 nm, similar to Exos (Figure 2(A)). The particle size of EM-Dox was slightly larger after doxorubicin-loading by nanoparticle tracking analysis (NTA) measurement, and EMs had a larger diameter than Exos (Figure 2(B)). We calculated the EMs and Exos yields of 1×10^7 cells. The protein content and particle number of EMs produced by it were about 200 μ g and 2×10^{12} particles, whereas the Exos produced by it were about 10 μ g and 1×10^{11} particles. Thus, the yield of EMs is about 20 times more than Exos (Figure 2(C,D)). Western blot analysis confirmed the expression of several exosomal markers, including CD63, Tsg101, and Alix in EMs (Figure 2(E)), which is identical to Exos. These results indicate that our engineered EMs feature a highly similar nanostructure and surface protein expression to Exos derived from the same BMSCs.

3.2. The encapsulation efficiency of doxorubicin

We used the ammonium sulfate gradient loading method to load doxorubicin. The active loading method has a high loading efficiency. We found that loading doxorubicin into EMs is strongly associated with the drug concentration initially added to EMs suspension. As shown in Figure 3(B), the 10^{10} /mL EMs was loaded with 0.2 mg/mL, 0.5 mg/mL, 0.8 mg/mL, and 1 mg/mL doxorubicin, respectively. The loading efficiency of EMs positively correlated with the concentration of doxorubicin in the solution and reached a peak at 0.8 mg/mL doxorubicin concentration.

3.3. The drug release profile of EMs

The drug release profile is a critical factor affecting the drug release process of EM *in vivo*. Thus, we investigated the *in vitro* drug release profile of EM-Dox. To simulate the endolysosomal compartment interior environment and normal physiological environment, the release profile of EM-Dox in PBS dialysate at pH 5.5 or 7.4 was determined (Figure 3(D)). After 48 h, approximately 80% of doxorubicin was released at pH 5.5. In comparison, only 60% of doxorubicin was released at pH 7.4. The results showed that the acidic environment could protonate doxorubicin and thus accelerate the release of doxorubicin. The drug release profile results indicate that the release of EM-Dox is triggered by the acidic environment (lysosomes of cancer cells), which proves the promising antitumor properties of EM-Dox.

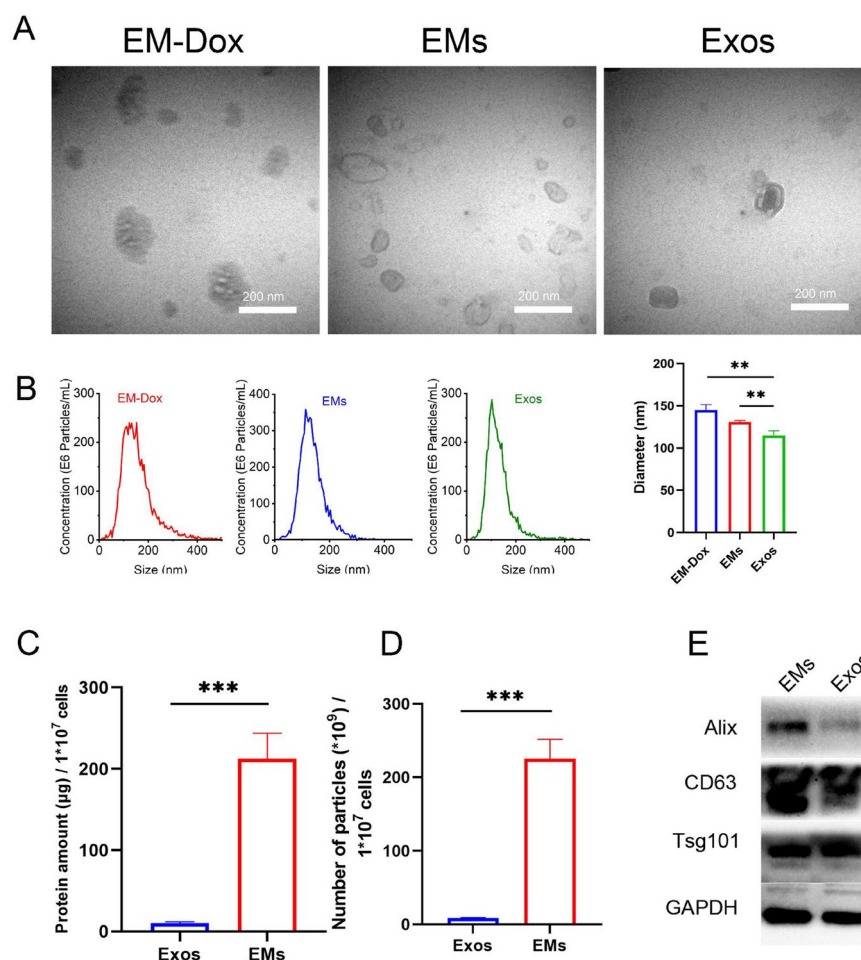


Figure 2. Characterization of EM-Dox, Exos, and EMs. **A:** TEM images of EM-Dox, Exos, and EMs. This image shows a typical structure of EM-Dox, Exos, and EMs (scale bar 200 nm). **B:** Size distributions of EM-Dox, Exos, and EMs. The yields of EMs and Exos measured as the total protein (**C**) and particle number (**D**) from 1×10^7 BMSCs. **E:** Characterization of Exos and EMs by ECL Western blotting. The positive exosomal markers Alix, CD63, and Tsg101. (* $p < .05$, ** $p < .01$, or *** $p < .001$).

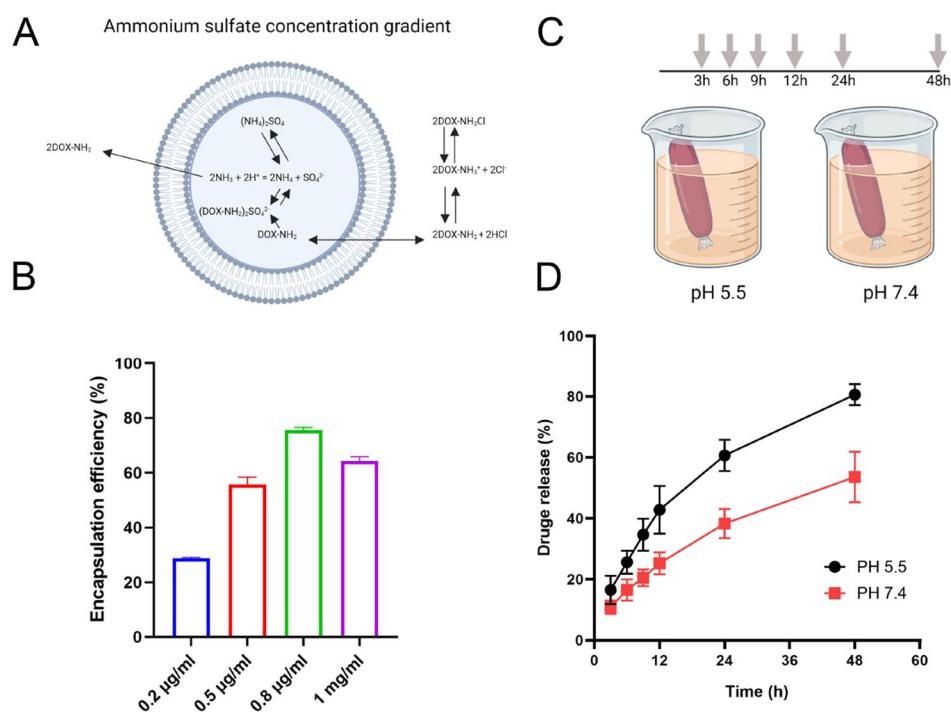


Figure 3. **A:** Ammonium sulfate transmembrane concentration gradient active load doxorubicin schematic. **B:** Encapsulation efficiency of EM-Dox in different doxorubicin concentrations. **C:** The release amount of doxorubicins at different time points. **D:** The drug release profile of EM-Dox in PBS with pH 7.4 and pH 5.5, respectively.

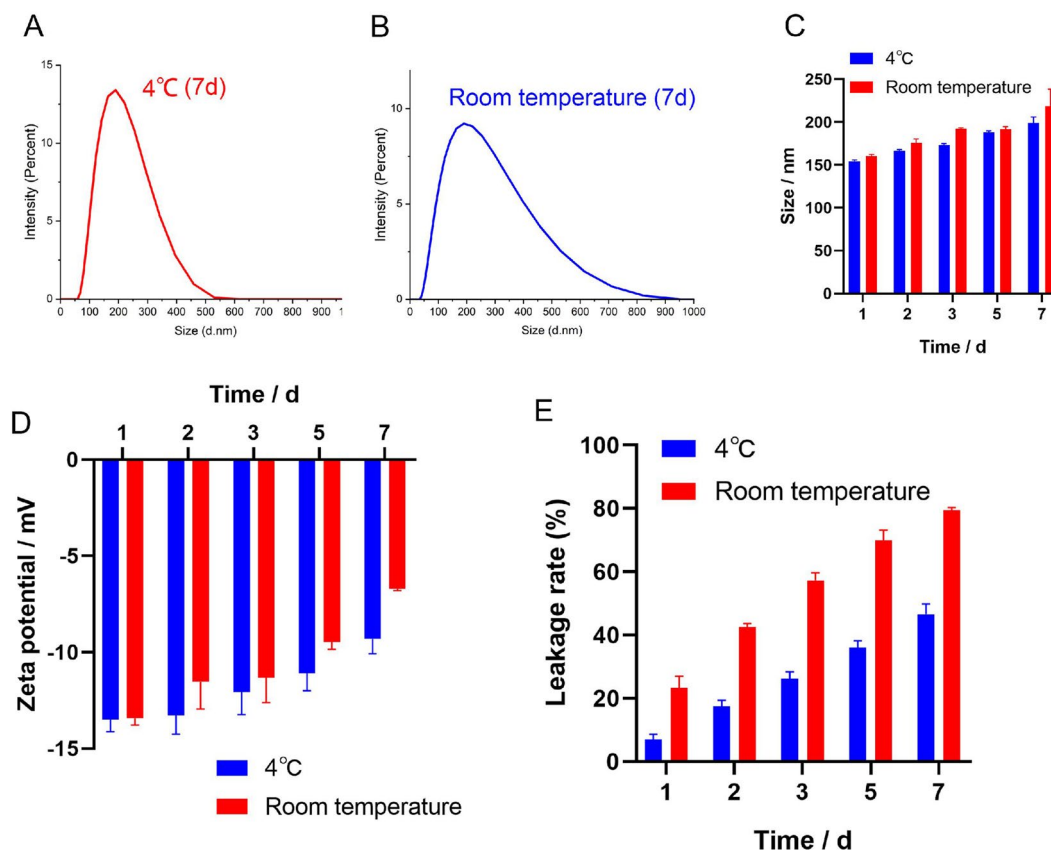


Figure 4. Effects of storage conditions on EM-Dox size and Dox leakage rate. A and B: DLS of enriched EM-Dox after storage at 4°C and room temperature. C: Average EM-Dox size change for each storage temperature. D: Average EM-Dox zeta potential change for each storage temperature. E: Dox leakage of EM-Dox for each storage temperature. (ns, not significant, * $p < .05$, ** $p < .01$, or *** $p < .001$).

3.4. Stability of nanosystem

We determined the effect of different storage temperatures on the size of EM-Dox. The peak values of EM-Dox size distribution after storage at 4°C and room temperature for 7 days were 199 ± 5.8 nm and 218.8 ± 16.1 nm, respectively (Figure 4(A,B)). The size of EM-Dox stored at 4°C and room temperature changed. In contrast, the size of EM-Dox stored at room temperature became larger (Figure 4(C)). Next, we compared the effect of storage conditions on the charge density distribution around EM-Dox. The average zeta potential of freshly prepared EM-Dox was -13.5 ± 0.4 mV. After storage at room temperature and 4°C, the zeta potential of EM-Dox showed a downward trend, and the decrease was more obvious at room temperature (Figure 4(D)). At the same time, we measured the doxorubicin leakage rate of EM-Dox at room temperature and at 4°C. The results showed that the leakage rate of the drug at room temperature was significantly higher than that at 4°C (Figure 4(E)). These experiments prove that the nanosystem in this study has good stability at low temperature.

3.5. The cellular uptake of EM-Dox in vitro

Confocal laser scanning microscopy (CLSM) was used to assess the cell uptake of EM-Dox. 143B cells or MG63 cells were co-incubated with PKH26-labeled EM-Dox at 37°C for 1, 6, and 9 h. Obtained confocal images showed that most

EM-Dox entered cells after 1-h incubation, and EMs (red) was co-localized with doxorubicin (green) (Figure 5). These results indicated that EMs and doxorubicin simultaneously enter osteosarcoma cells via endocytotic pathways.

3.6. The cytotoxicity and antitumor effects of EM-Dox in vitro

The antitumor activity of engineered EM-Dox was determined. The EM-Dox was co-incubated with 143B or MG63 cells (0–15 $\mu\text{g}/\text{mL}$) for 24 h. The cytotoxicity of EM-Dox to osteosarcoma cells 143B or MG63 was detected by cell counting Kit-8 (CCK-8) cell viability assay. As shown in Figure 6, the semi-inhibitory concentrations (IC₅₀) of EM-Dox for 143B and MG63 cells were determined as 1.8 $\mu\text{g}/\text{mL}$ and 3.72 $\mu\text{g}/\text{mL}$, respectively. The IC₅₀ of free Dox for 143B and MG63 cells were determined as 5.07 $\mu\text{g}/\text{mL}$ and 5.53 $\mu\text{g}/\text{mL}$, respectively (Figure 6(A,B)). The inhibitory concentration of EM-Dox on 143B was better than that of free doxorubicin, but this phenomenon was not observed in MG63.

3.7. PK of EM-Dox in plasma

The concentration of doxorubicin in plasma of rats treated with EM-Dox was detected by HPLC. The plasma concentration–time curve of doxorubicin is shown in Figure 7. PK parameters were evaluated by non-compartment model. After

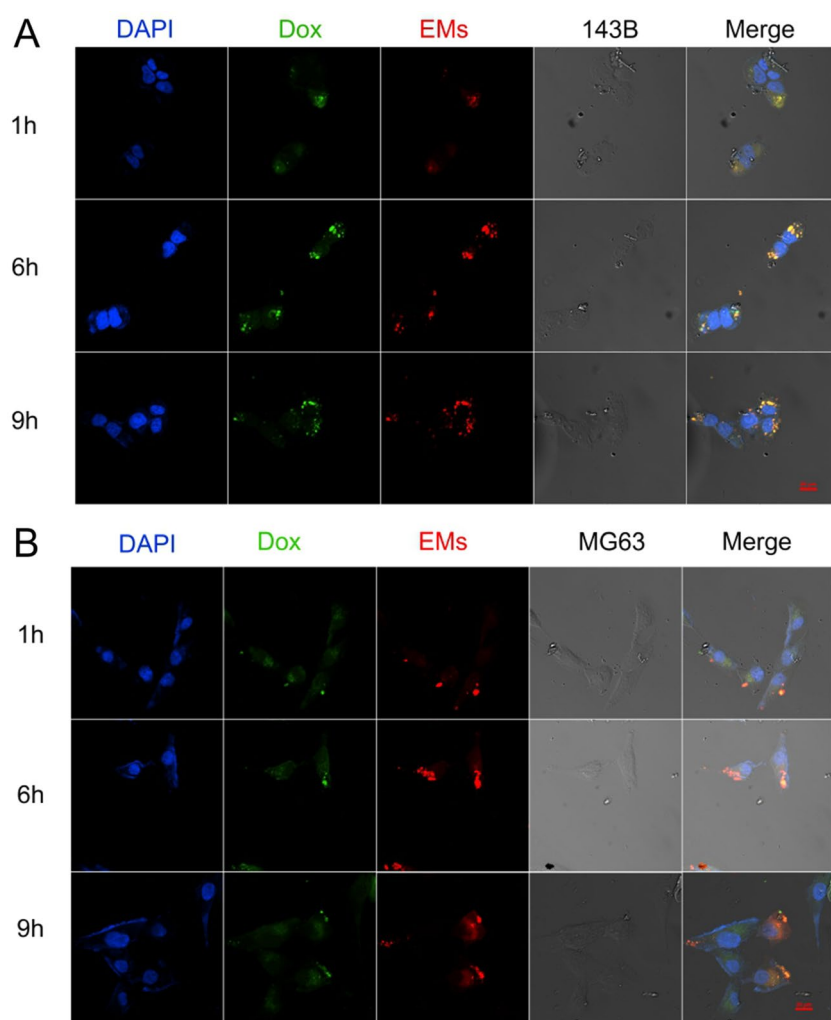


Figure 5. Representative fluorescent microscope images show the distribution of EM-Dox after 1, 6, and 9 h in 143B (A) and MG63 (B); the scale bar was 20 μm .

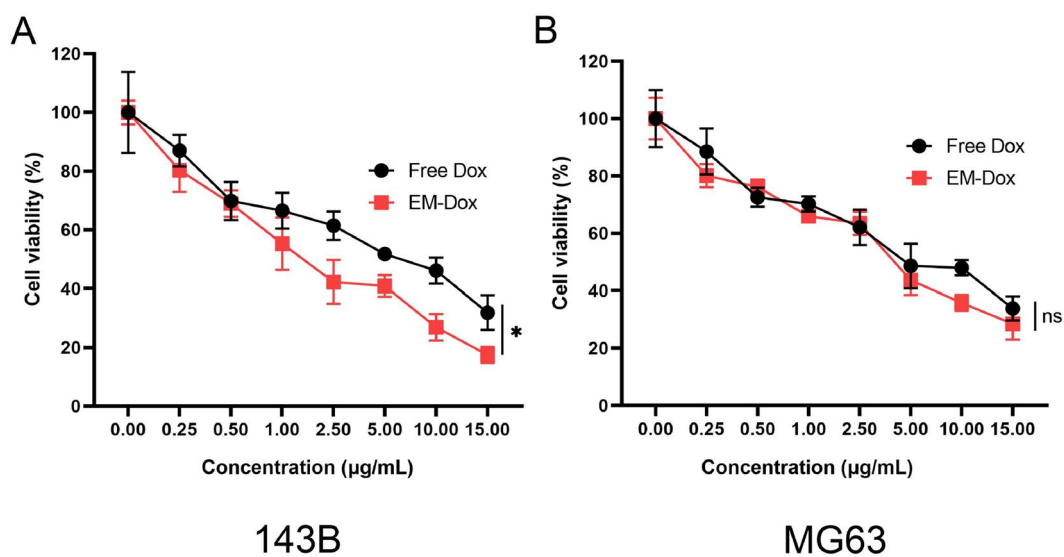


Figure 6. Cytotoxic activity of EM-Dox in 143B (A) and MG63 (B) osteosarcoma cells. (* $p < 0.05$).

an intravenous injection of 3 mg/kg of EM-Dox, the PK profile showed that Clearance (CL) was $67.17 \pm 4.12 \text{ mL/h}$ and V was $1537.99 \pm 474.71 \text{ mL}$. AUC_{last} was $66,601.13 \pm 3287.25 \text{ ng h/mL}$, and $T_{1/2}$ was $16 \pm 5.44 \text{ h}$. The maximum plasma doxorubicin

concentration (C_{max}) was observed at 30 min after EM-Dox injection. The concentration decreased rapidly within 8 h, followed by a slow distribution phase and a final elimination phase.

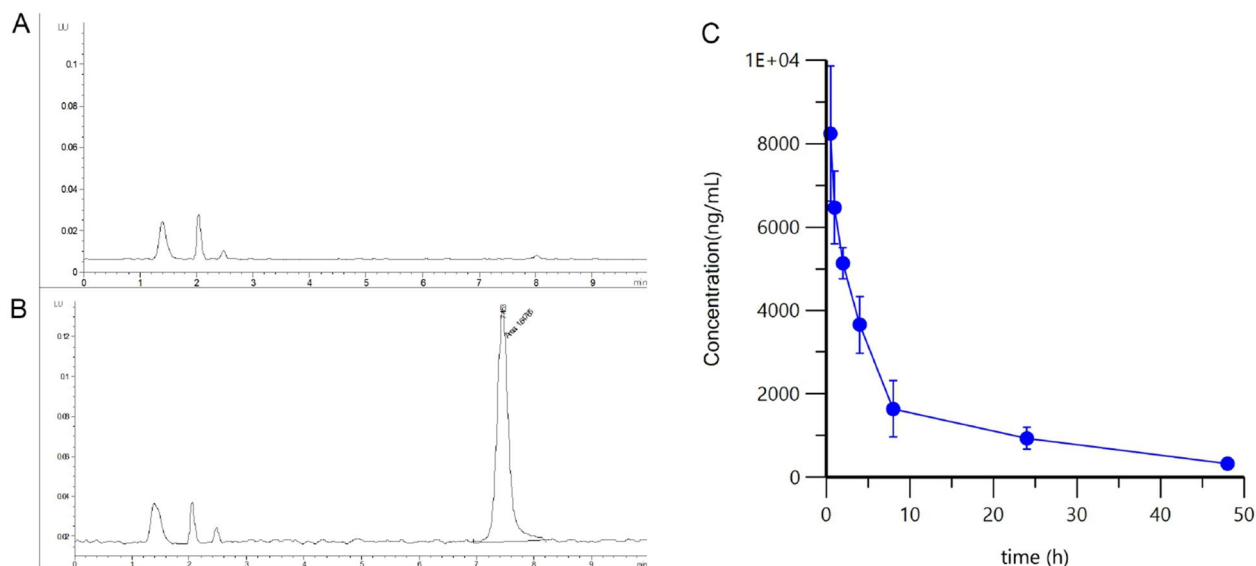


Figure 7. The chromatograms of EM-Dox and the concentration–time profiles of EM-Dox in plasma after EM-Dox administration. A: A blank plasma sample without EM-Dox; (B) a real plasma sample collected after intravenous administration of 3 mg/kg EM-Dox 24 h. C: Concentration–time curve of EM-Dox after 3 mg/kg of EM-Dox administration.

3.8. *In vivo* biodistribution experiment

Near infrared fluorescence (NIR) fluorescence imaging was used to study the organ distribution and tumor accumulation of EMs in the BALB/c nude mice model. IVIS was used to measure the fluorescence images of mice at 6, 24, and 48 h after injection (Figure 8(A)). The results showed that EMs had rapidly reached the tumor site at 6 h, while no obvious tumor accumulation was observed in liposomes. In addition, the accumulation of EMs and liposomes reached the maximum after 24 h, and the fluorescence intensity of EMs was higher. After 48 h, it could be seen that EMs were still accumulated in the tumor (Figure 8(B)), suggesting that EMs had a long circulation time in the body. After 48 h, the *in vitro* fluorescence intensity of the tumor still showed that EMs accumulated more in the tumor than liposomes (Figure 8(C)). In addition, the fluorescence of EMs in various organs was higher than that of liposomes (Figure 8(D)). However, the difference in fluorescence between organs was small, and tumor aggregation was significantly different.

3.9. *In vivo* therapeutic activity of EM-Dox

We evaluated the antitumor activity of EM-Dox in a BALB/c nude mice model of osteosarcoma. Mice were randomly divided into four groups, with six tumors in each group. The first group was injected with EM-Dox (3 mg/kg), the second group was injected with free Dox (3 mg/kg), the third group was injected with blank EMs (3 mg/kg), and the fourth group was injected with PBS as control. Treatments were administered every three days for a total of four times (Figure 9(A)). After each injection, the mice were weighed, and their tumor volumes were measured every other day. As shown in Figure 9(B), the tumor growth of mice injected with EM-Dox was slow, followed by mice injected with free doxorubicin. There was no significant difference in tumor growth between mice

injected with EMs and PBS (Figure 9(D)). The mouse bodyweights show no significant difference between each group (Figure 9(E)). After treatment, the mice were sacrificed, and the tumor-bearing hind limbs were weighed. The results showed that the tumor volume of mice in the EM-Dox group was the smallest and significantly lower than that in the free doxorubicin group (Figure 7(C)).

We tested the blood toxicity of the mice treated with EM-Dox and controls, including liver function, kidney function, and myocardial enzyme. CK and LDH in the free doxorubicin group were significantly higher than those in the control group but not in the EM-Dox group (Figure 10(A,B)), suggesting that EMs can protect the heart functions of mice. Still, the liver toxicity biomarker levels (AST or ALT) of the free doxorubicin group were significantly higher than that of the EM-Dox group (Figure 10(C,D)), proving that EM-based doxorubicin delivery can protect the liver. There was no significant difference in the renal function between each group (Figure 10(E,F)). These *in vivo* efficacy results showed that EM-Dox was efficient and safe for treating primary osteosarcoma.

4. Discussion

In clinical practice, chemotherapy is an indispensable treatment for patients with osteosarcoma. Nevertheless, the off-target toxicity significantly limits the dose of chemotherapy drugs, resulting in high mortality in patients with osteosarcoma. Nanoscale drug delivery systems (NanoDDSs) can accurately deliver chemotherapeutic drugs to the tumor area, thereby increasing the tumor accumulation of drugs and reducing off-target toxicity. At present, synthetic nanoDDSs (e.g. polymeric nanoparticles or liposomes) are widely used in drug encapsulation and delivery.

Zheng et al. (2019) used nanoparticles of poly(ferulic acid) to deliver doxorubicin to treat cancer and achieved good

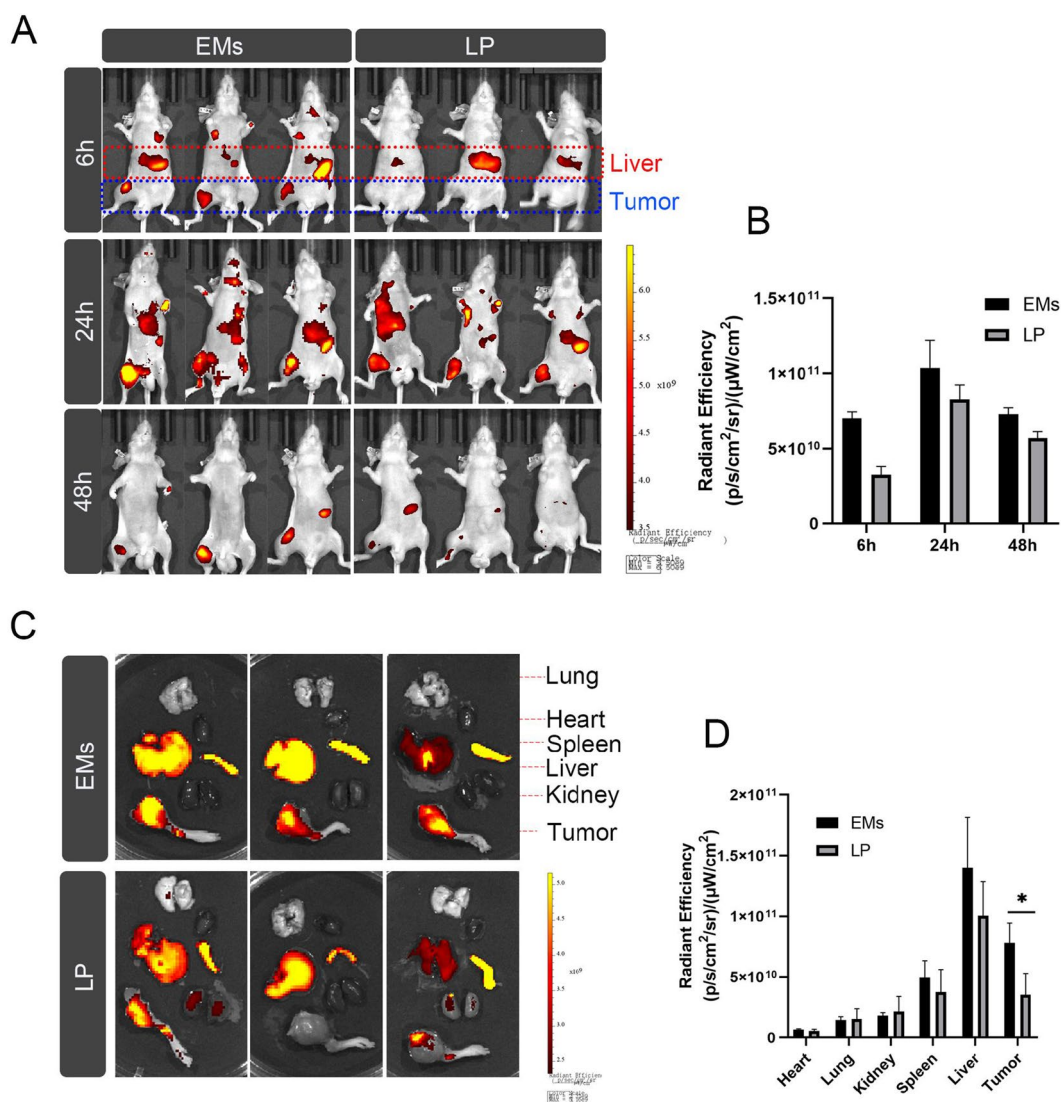


Figure 8. *In vivo* biodistribution of EMs. A: NIR fluorescent images of mice at 6, 24, 48 h after injection ($n=3$ per group). B: Quantified tumor accumulation of EMs or LP. C: Representative *ex vivo* biodistribution of EMs or LP (lung, heart, liver, spleen, kidney, and tumor). D: Fluorescence quantification of organs. (* $p < .05$). LP, lipidosome.

results. A phase I study showed that Selinexor, a selective inhibitor of nuclear export, combined with high-dose dexamethasone, ifosfamide, terminator, and etoposide (DICE) in the treatment of relapsed/refractory (R/R) T-cell lymphoma (TCL) and natural-killer/T-cell lymphoma (NKTL) showed promising complete remission rates (Tang et al., 2021). However, these synthetic nanocarriers are limited by immunogenicity, toxicity, and drug delivery efficiency. Exos are endogenous nanoscale extracellular vesicles with significantly lower immunogenicity than synthetic nanocarriers (Kamerkar et al., 2017). Many studies have used Exos as a carrier to deliver chemotherapy drugs for tumor diagnosis or treatment (Zhuang et al., 2011; Hu et al., 2015; Kim et al., 2016; Srivastava et al., 2016). However, the low yield after the purification of Exos limits its development as a biological nanoDDS. Jang et al. (2013) used the sequential extrusion method to prepare EMs for the first time, its production was 100 times higher than that of traditional exosome extraction, and the EMs retained the intrinsic tumor targeting. Subsequently, Goh et al. (2017) also produced exosome mimetics to encapsulate doxorubicin, which

has a natural targeting ability to tumors. In this study, we successfully prepared BMSC-derived EMs by sequential extrusion and encapsulated doxorubicin to produce EM-Dox. In the *in vivo* experiments, EM-Dox showed obvious anti-tumor effects. In addition, EM-Dox has reduced heart and liver toxicities compared with free doxorubicin. Our results suggest that EMs derived from BMSC are an effective drug delivery carrier.

In this study, we measured and characterized the shape, size, and membrane characteristic proteins of the produced EMs, Exos, and EM-Dox. The results showed that EMs, Exos, and EM-Dox were uniformly distributed and had good stability at -80°C . The larger EMs compared to Exos provided good conditions for drug loading. After loading doxorubicin, the size of EM-Dox became larger, but the particle size was still mostly distributed in the range of 30–200 nm, which still had good biodistribution and permeability. We compared the protein and particle yields of EMs and Exos and found that EMs was about 20 times higher than Exos. In addition, EMs and Exos have similar characteristics, which prove that

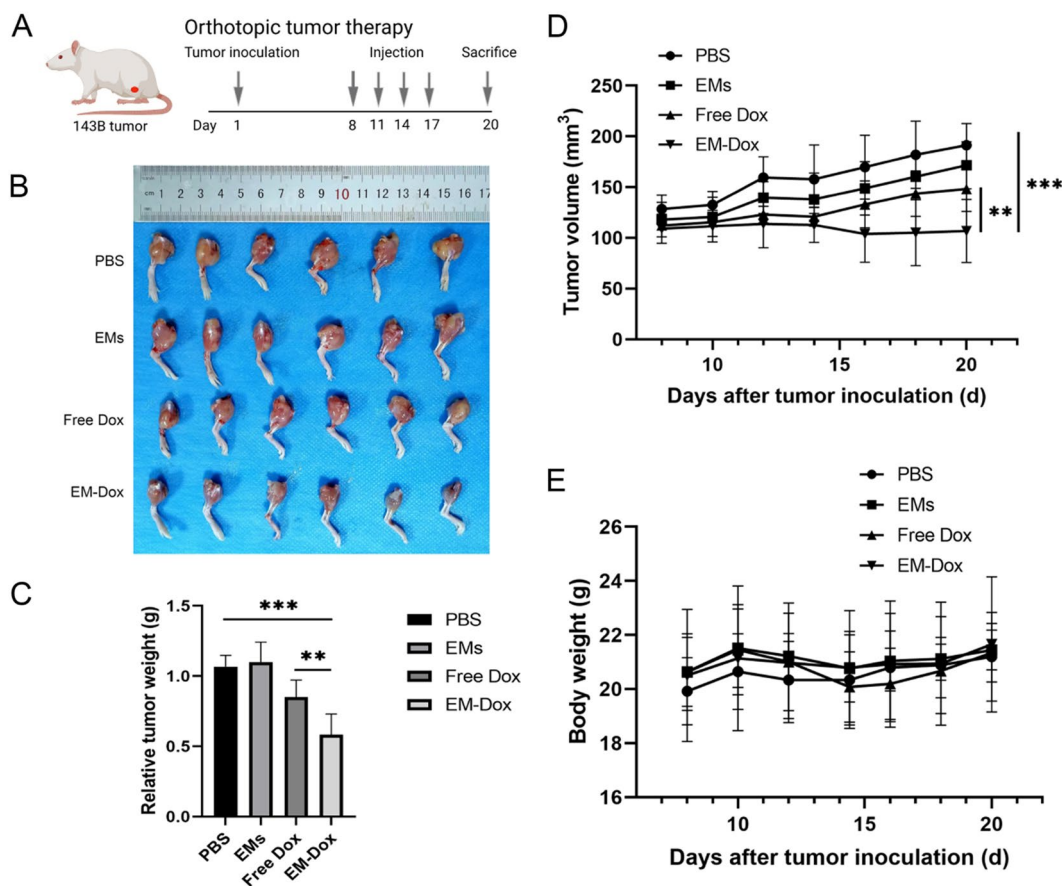


Figure 9. Therapeutic effects of EM-Dox *in vivo*. A: The timeline of the orthotopic tumor therapy model. B: The images of excised orthotopic 143B tumors from mice ($n=6$ per group) treated with PBS, EMs, free Dox, or EM-Dox. C: Tumorous hind limbs at the endpoint were quantified by weight. D: Tumor progression was measured by a caliper. EM-Dox dramatically inhibit tumor growth. E: No significant difference was shown in mouse body weight during the treatment. (** $p < .01$, or *** $p < .001$). Dox, doxorubicin; EM-Dox, doxorubicin-loaded exosome mimetics.

we successfully prepared the substitute for Exos and greatly improved the yield.

In addition, compared with traditional methods such as electroporation, ultrasound, freeze-thaw, and passive incubation, active drug loading method using ammonium sulfate gradient significantly improved the doxorubicin encapsulation efficiency (Chen et al., 2021). Barenholz (2012) used an active drug delivery method driven by a transmembrane ammonium sulfate gradient to encapsulate doxorubicin in liposomes, which was eventually successfully used in the clinic. In the study, we applied this highly efficient active loading method for EM payload encapsulation driven by ammonium sulfate gradient across membranes (Figure 3(A)). Specifically, we used 240 mM ammonium sulfate solution to replace PBS in the centrifuge extruded cell suspension after extruding twice, causing EMs to produce a transmembrane concentration gradient. In conjunction with the dialysis step, doxorubicin molecules can be actively loaded into EMs. Our encapsulating method can close the drug loading rate to 80%, ensuring that doxorubicin is encapsulated efficiently by EMs. In this study, cells were re-suspended in an ammonium sulfate solution, which promoted ammonium sulfate to enter EMs during extrusion. They then formed a gradient of ammonium sulfate inside and outside EMs vesicles through dialysis to actively promote doxorubicin to enter EMs. However, this is not easy to be achieved in natural Exos. Ammonium sulfate can be easily loaded into

vesicles during the extrusion of EMs, but natural Exos require an additional route for loading ammonium sulfate. For example, Chen et al. (2021) used sonication and extrusion-assisted active loading to promote ammonium sulfate into vesicles. Our approach is relatively simple and efficient. Therefore, our method encapsulated doxorubicin efficiently.

Next, we verified the killing ability of EM-Dox on osteosarcoma cells *in vitro*. EMs successfully delivered doxorubicin to 143B and MG63 osteosarcoma cells in cellular uptake experiments. Drug release experiments also proved that EM-Dox is more likely to release doxorubicin to kill osteosarcoma cells in the acidic environment of tumor lysosomes. Our results are similar to other drug delivery systems, with faster drug release in acidic environments (Li et al., 2020; Liu et al., 2021). In addition, similar to previous studies, the release of EM-Dox in physiological environments is lower than that of doxorubicin encapsulated in natural exosomes, demonstrating another advantage of EMs as a carrier (Goh et al., 2017; Wu et al., 2021). In the cytotoxicity experiment, EM-Dox showed strong cytotoxicity against osteosarcoma cells. Moreover, in 143B cells, the cytotoxicity of EM-Dox was slightly higher than that of free doxorubicin. The results of *in vitro* experiments showed that EM-Dox could effectively kill osteosarcoma cells.

Encouraged by the *in vitro* experiment, we first used NIR fluorescence imaging to detect the distribution of EMs *in*

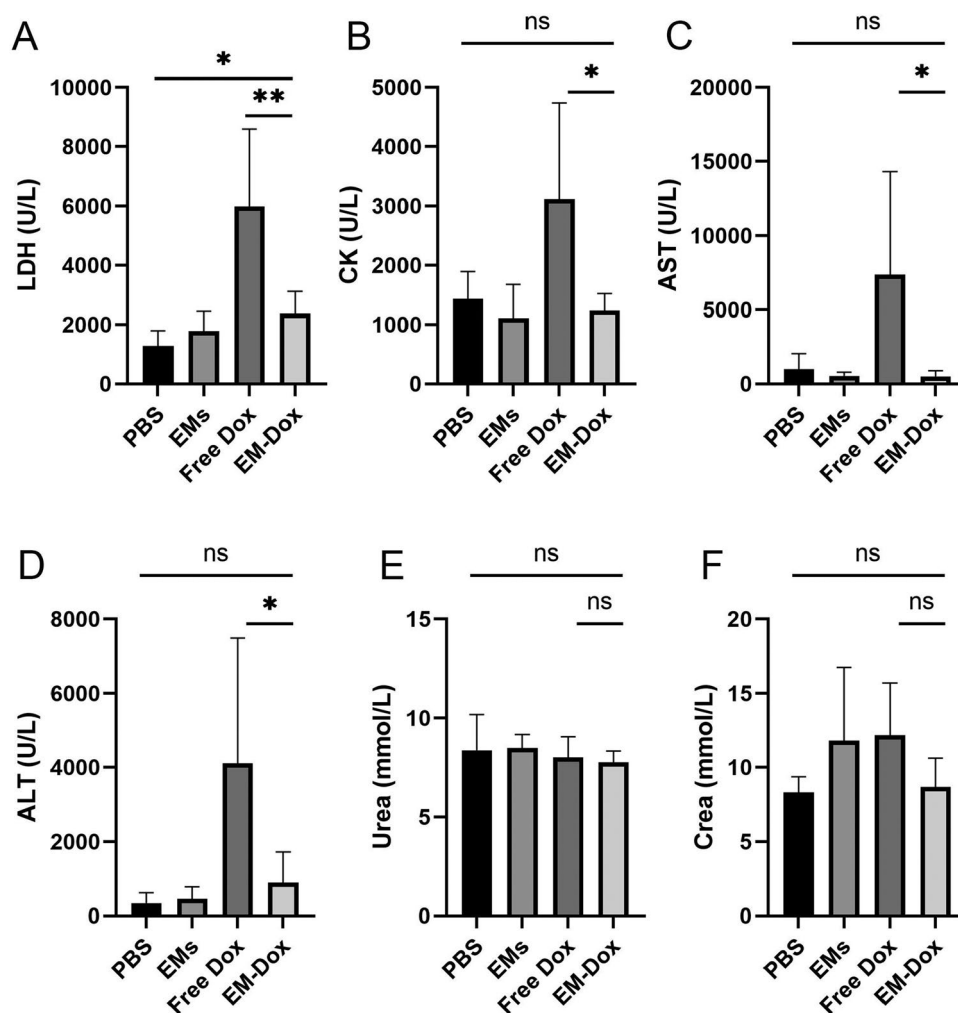


Figure 10. A and B: After treatments, creatine kinase (CK) and lactate dehydrogenase (LDH) levels in mice. C and D: ALT and AST levels in mice after treatments. E and F: Urea and Crea levels in mice after treatments. (ns, not significant, * $p < .05$, or ** $p < .01$).

in vivo and the aggregation of EMs in tumors. The results showed that EMs could accumulate in the tumor faster and longer. Finally, although fluorescence quantitatively showed that EMs gathered more in various organs, the difference was small, suggesting that the biological distribution of EMs and liposomes was similar. However, the aggregation of EMs in tumor was significantly higher than that of liposomes, suggesting that EMs has a good tumor aggregation effect.

Then, we used EM-Dox to treat osteosarcoma tumor-bearing mice. We compared the tumor inhibitory effects of EM-Dox with free doxorubicin and used empty EMs and PBS as control groups. The results showed that EM-Dox had stronger inhibitory effect on osteosarcoma tumor than free doxorubicin. The empty EMs without doxorubicin showed no significant tumor inhibition compared with the PBS group, indicating that BMSC-derived EMs can be safely used as an effective nanocarrier to deliver doxorubicin in the treatment of osteosarcoma. The main side effect of doxorubicin is cardiotoxicity (Wenningmann et al., 2019), which limits the maximum dose of doxorubicin. Previous studies have shown that exosome-encapsulated doxorubicin has higher cardiac safety (Wei et al., 2019). Exosome-encapsulated doxorubicin can be precisely delivered into the tumor sites, with less accumulation in normal tissues, leading to a higher safe dose. In

addition, EMs was also used to encapsulate doxorubicin to reduce cardiac toxicity (Wu et al., 2021). In other words, EM-Dox reduces drug distribution in the heart, thereby increasing the maximum dose available to patients. Our results showed that the serum LDH and CK levels of EM-Dox treated mice were lower than those of free doxorubicin. That is, EMs delivers doxorubicin effectively, increasing tumor inhibition while reducing cardiac aggregation. There was no significant difference in the weight of mice among groups. It is different from the previous study (Wei et al., 2019), the levels of serum AST and ALT in mice treated with EM-Dox, EMs, and PBS were not significantly increased, while those in mice treated with free doxorubicin increased. In addition, there was no significant difference in urea nitrogen, serum creatinine, white blood cells, red blood cells, and platelets among mice in each group. In summary, the anti-tumor effect of EM-Dox on osteosarcoma tumor-bearing nude mice was enhanced, with reduced off-target toxicities.

5. Conclusion

In this study, we used BMSCs to generate EMs by sequential extrusion, and successfully encapsulated doxorubicin by an

ammonium sulfate gradient method. Our engineered EM-Dox demonstrates excellent antitumor properties both *in vivo* and *in vitro*, leading to better tumor-specificity and biocompatibility compared with the free doxorubicin. EMs derived from BMSCs represent an excellent biological nanocarrier for chemodrug delivery in osteosarcoma treatment. In order to further study, we plan to compare EMs with artificial nanomaterials to further explore the advantages of EMs as a promising biological nanomedicine.

Authors' contributions

DWH, JKW, and MJL designed the study; DWH designed and guided the project; XJT, CHZH, JKW, JYL, MJL, LJ and PG collected and analyzed the data; JKW and MJL drafted the initial manuscript; GHW, CHZH, TM, JYL, ZXZ and DWH revised the article critically; XW, ZXZ, JYL, DWH, MJL and PG reviewed and edited the article. All authors approved the final manuscript.

Disclosure statement

The authors declare that they have no competing interests.

Funding

This study was supported by Special Key Project of Chongqing Technology Innovation and Application Development (No. Cstc2019jscx-tjsbX0003).

References

- Alvarez-Erviti L, Seow Y, Yin H, et al. (2011). Delivery of siRNA to the mouse brain by systemic injection of targeted exosomes. *Nat Biotechnol* 29:341–5. Epub 2011 Mar 20. PMID: 21423189.
- Anninga JK, Gelderblom H, Fiocco M, et al. (2011). Chemotherapeutic adjuvant treatment for osteosarcoma: where do we stand? *Eur J Cancer* 47:2431–45. Epub 2011 Jun 22. PMID: 21703851.
- Barenholz Y. (2012). Doxil®—the first FDA-approved nano-drug: lessons learned. *J Control Release* 160:117–34. Epub 2012 Mar 29. PMID: 22484195.
- Chen C, Sun M, Wang J, et al. (2021). Active cargo loading into extracellular vesicles: highlights the heterogeneous encapsulation behaviour. *J Extracell Vesicles* 10:e12163. PMID: 34719860; PMCID: PMC8558234.
- Colao IL, Corteling R, Bracewell D, Wall I. (2018). Manufacturing exosomes: a promising therapeutic platform. *Trends Mol Med* 24:242–56. Epub 2018 Feb 12. PMID: 29449149.
- Freyer DR, Seibel NL. (2015). The clinical trials gap for adolescents and young adults with cancer: recent progress and conceptual framework for continued research. *Curr Pediatr Rep* 3:137–45. Epub 2015 Feb 18. PMID: 30613438; PMCID: PMC6319956.
- Goh WJ, Lee CK, Zou S, et al. (2017). Doxorubicin-loaded cell-derived nanovesicles: an alternative targeted approach for anti-tumor therapy. *Int J Nanomed* 12:2759–67. PMID: 28435256; PMCID: PMC5388236.
- Goh WJ, Zou S, Ong WY, et al. (2017). Bioinspired cell-derived nanovesicles versus exosomes as drug delivery systems: a cost-effective alternative. *Sci Rep* 7:14322. PMID: 29085024; PMCID: PMC5662560.
- Gomari H, Forouzandeh Moghadam M, Soleimani M, et al. (2019). Targeted delivery of doxorubicin to HER2 positive tumor models. *Int J Nanomed* 14:5679–5690. Erratum in: *Int J Nanomed* (2019). 14:7919. PMID: 31413568; PMCID: PMC6662522.
- Guo P, Busatto S, Huang J, et al. (2021). A facile magnetic extrusion method for preparing endosome-derived vesicles for cancer drug delivery. *Adv Funct Mater* 31:2008326. Epub 2021 Jan 20. PMID: 34924915; PMCID: PMC8680268.
- Hu L, Wickline SA, Hood JL. (2015). Magnetic resonance imaging of melanoma exosomes in lymph nodes. *Magn Reson Med* 74:266–71. Epub 2014 Jul 22. PMID: 25052384; PMCID: PMC4422779.
- Jaffe N. (2009). Osteosarcoma: review of the past, impact on the future. *The American experience*. In: Jaffe N, Bruland OS, Bielack S, eds. *Pediatric and adolescent osteosarcoma*. Boston: Springer, 239.
- Jang SC, Kim OY, Yoon CM, et al. (2013). Bioinspired exosome-mimetic nanovesicles for targeted delivery of chemotherapeutics to malignant tumors. *ACS Nano* 7:7698–710. Epub 2013 Sep 4. Erratum in: *ACS Nano* (2014). 8:1073. PMID: 24004438.
- Jiang L, Vader P, Schifflers RM. (2017). Extracellular vesicles for nucleic acid delivery: progress and prospects for safe RNA-based gene therapy. *Gene Ther* 24:157–66. Epub 2017 Jan 31. PMID: 28140387.
- Kamerkar S, LeBleu VS, Sugimoto H, et al. (2017). Exosomes facilitate therapeutic targeting of oncogenic KRAS in pancreatic cancer. *Nature* 546:498–503. Epub 2017 Jun 7. PMID: 28607485; PMCID: PMC5538883.
- Kim MS, Haney MJ, Zhao Y, et al. (2016). Development of exosome-encapsulated paclitaxel to overcome MDR in cancer cells. *Nanomedicine* 12:655–64. Epub 2015 Nov 14. PMID: 26586551; PMCID: PMC4809755.
- Li S, Wang X. (2021). The potential roles of exosomal noncoding RNAs in osteosarcoma. *J Cell Physiol* 236:3354–65. Epub 2020 Oct 12. PMID: 33044018.
- Li S, Zhang T, Xu W, et al. (2018). Sarcoma-targeting peptide-decorated polypeptide nanogel intracellularly delivers shikonin for upregulated osteosarcoma necroptosis and diminished pulmonary metastasis. *Theranostics* 8:1361–1375. Erratum in: *Theranostics* (2020). 10:5530–1. PMID: 29507626; PMCID: PMC5835942.
- Li X, Wang L, Wang L, et al. (2020). Overcoming therapeutic failure in osteosarcoma via Apatinib-encapsulated hydrophobic poly(ester amide) nanoparticles. *Biomater Sci* 8:5888–99. PMID: 33001086.
- Li Z, Huang J, Du T, et al. (2022). Targeting the Rac1 pathway for improved prostate cancer therapy using polymeric nanoparticles to deliver of NSC23766. *Chin Chem Lett* 33:2496–500.
- Liu Y, Qiao Z, Gao J, et al. (2021). Hydroxyapatite-bovine serum albumin-paclitaxel nanoparticles for locoregional treatment of osteosarcoma. *Adv Healthc Mater* 10:e2000573. Epub 2020 Nov 9. PMID: 33166086.
- Liu Y, Xia Y, Smollar J, et al. (2021). The roles of small extracellular vesicles in lung cancer: Molecular pathology, mechanisms, diagnostics, and therapeutics. *Biochim Biophys Acta Rev Cancer* 1876:188539. Epub 2021 Apr 20. PMID: 33892051.
- Meyers PA. (2015). Systemic therapy for osteosarcoma and Ewing sarcoma. *Am Soc Clin Oncol Educ Book* e644-7. PMID: 25993235.
- Reiner AT, Witwer KW, van Balkom BWM, et al. (2017). Concise review: developing best-practice models for the therapeutic use of extracellular vesicles. *Stem Cells Transl Med* 6:1730–9. Epub 2017 Jul 17. PMID: 28714557; PMCID: PMC5689784.
- Shu S, Yang Y, Allen CL, et al. (2020). Purity and yield of melanoma exosomes are dependent on isolation method. *J Extracell Vesicles* 9:1692401. PMID: 31807236; PMCID: PMC6882439.
- Song H, Zhao J, Cheng J, et al. (2021). Extracellular vesicles in chondrogenesis and cartilage regeneration. *J Cell Mol Med* 25:4883–92. Epub 2021 May 4. PMID: 33942981; PMCID: PMC8178250.
- Srivastava A, Amreddy N, Babu A, et al. (2016). Nanosomes carrying doxorubicin exhibit potent anticancer activity against human lung cancer cells. *Sci Rep* 6:38541. PMID: 27941871; PMCID: PMC5150529.
- Tang T, Martin P, Somasundaram N, et al. (2021). Phase I study of selinexor in combination with dexamethasone, ifosfamide, carboplatin, etoposide chemotherapy in patients with relapsed or refractory peripheral T-cell or natural-killer/T-cell lymphoma. *Haematologica* 106:3170–5. PMID: 33147935; PMCID: PMC8634181.
- van Niel G, D'Angelo G, Raposo G. (2018). Shedding light on the cell biology of extracellular vesicles. *Nat Rev Mol Cell Biol* 19:213–28. Epub 2018 Jan 17. PMID: 29339798.

- Wei H, Chen J, Wang S, et al. (2019). A nanodrug consisting of doxorubicin and exosome derived from mesenchymal stem cells for osteosarcoma treatment in vitro. *Int J Nanomed* 14:8603–10. PMID: 31802872; PMCID: PMC6830377.
- Wenningmann N, Knapp M, Ande A, et al. (2019). Insights into doxorubicin-induced cardiotoxicity: molecular mechanisms, preventive strategies, and early monitoring. *Mol Pharmacol* 96:219–32. Epub 2019 Jun 4. PMID: 31164387.
- Wu JY, Li YJ, Hu XB, et al. (2021). Exosomes and biomimetic nanovesicles-mediated anti-glioblastoma therapy: a head-to-head comparison. *J Control Release* 336:510–21. Epub 2021 Jul 6. PMID: 34237399.
- Wu K, Yu B, Li D, et al. (2022). Recent advances in nanoplatfoms for the treatment of osteosarcoma. *Front Oncol* 12:805978. PMID: 35242707; PMCID: PMC8885548.
- Zhang XB, Zhang RH, Su X, et al. (2021). Exosomes in osteosarcoma research and preclinical practice. *Am J Transl Res* 13:882–97. PMID: 33841628; PMCID: PMC8014357.
- Zheng Y, You X, Chen L, et al. (2019). Biotherapeutic nanoparticles of poly(ferulic acid) delivering doxorubicin for cancer therapy. *J Biomed Nanotechnol* 15:1734–43. PMID: 31219014.
- Zhu Q, Ling X, Yang Y, et al. (2019). Embryonic stem cells-derived exosomes endowed with targeting properties as chemotherapeutics delivery vehicles for glioblastoma therapy. *Adv Sci (Weinh)* 6:1801899. PMID: 30937268; PMCID: PMC6425428.
- Zhuang X, Xiang X, Grizzle W, et al. (2011). Treatment of brain inflammatory diseases by delivering exosome encapsulated anti-inflammatory drugs from the nasal region to the brain. *Mol Ther* 19:1769–79. Epub 2011 Sep 13. Erratum in: *Mol Ther* (2012). 20:239. PMID: 21915101; PMCID: PMC3188748.